Colon Centreline Calculation for CT Colonography using Optimised 3D Topological Thinning

Robert J.T. Sadleir and Paul F. Whelan
Vision Systems Laboratory, School of Electronic Engineering,
Dublin City University, Dublin 9, Ireland.
{Robert.Sadleir, Paul.Whelan}@eeng.dcu.ie

Abstract

CT colonography is an emerging technique for colorectal cancer screening. This technique facilitates non-invasive imaging of the colon interior by generating virtual reality models of the colon lumen. Manual navigation through these models is a slow and tedious process. It is possible to automate navigation by calculating the centreline of the colon lumen. There are numerous well documented approaches for centreline calculation. Many of these techniques have been developed as alternatives to 3D topological thinning which has been discounted by others due to its computationally intensive nature. This paper describes a fully automated, optimised version of 3D topological thinning that has been specifically developed for calculating the centreline of the human colon.

1. Introduction

Colorectal cancer is a major cause of cancer related death in developed countries. Statistics published by the *National Cancer Registry of Ireland* (NCRI) [8] indicate that colon cancer accounted for 9% of all cancer cases diagnosed in Ireland in 1997, second only to non-melanoma skin cancer (36%). Regular screening has been demonstrated to reduce mortality from colorectal cancer. Conventional colonoscopy is the most sensitive screening technique that is currently available. Unfortunately there are several problems associated with conventional colonoscopy, it is highly invasive, requires sedation and has achieved limited acceptance among the those at risk of developing colorectal cancer.

CT colonography (CTC) [12] (also known as *virtual colonoscopy* (VC)) is an emerging technique for imaging the interior of the colon in a noninvasive manner. Using this technique, a suitably prepared patient undergos an abdominal CT scan. 3D virtual reality models of the colon are then generated and inspected in a manner similar to conventional colonscopy. Manual navigation through a virtual reality model of the colon is both time consuming and awkward. It is possible to automate intraluminal navigation by calculating the centreline of the colon. A large number of centreline calculation algorithms are described in the literature (see Section 2). This paper describes a novel alternative for centreline calculation. Initial tests have been carried out using real patient datasets and results indicate that our approach is a viable alternative for fast colon centreline calculation.

2. Previous Work

Early techniques for centreline calculation required significant user interaction. McFarland et al. [7] describe a semiautomated technique where a radiologist identifies key points in the colon lumen. A cubic spline fit of these points is then calculated to approximate the colon centreline. Samara et al. [9] calculate the colon centreline using the centre of mass of grown voxels. The plane perpendicular to each point in the centreline is determined and the centroid of lumen voxels is calculated for each plane. The set of centroid points is ultimately used to represent the centreline. Chiou et al. [3] and Bitter et al. [1] use centreline calculation techniques based on distance field analysis. These techniques, as well as others described in the literature, are compared in Table 1.

3. Segmentation

The centreline calculation algorithm described in this paper requires a binary model of the air insufflated colon lumen. A CTC dataset contains an extremely large amount of information. A segmented representation of the binary colon lumen must be obtained to facilitate centreline calculation. The majority of segmentation techniques utilise seeded 3D region growing where the initial seed point(s)

Proceedings of the First International Symposium on 3D Data Processing Visualization and Transmission (3DPVT'02)
0-7695-1521-5/02 $17.00 © 2002 IEEE

Group	Year	Technique	Platform	CPU(Mhz)	RAM(MB)	Automatic	Time(s)
Deschamps & Cohen [4]	2001	Distance field	Sun	300	1024	✗	30
Bitter et al. [1]	2001	Distance field	Intel	1000	NA	✓	119
Chen et al. [2]	2000	Distance field	SGI	2x195	896	✗	36
Samara et al. [9]	1999	Region Growing	SGI	NA	NA	✗	300
Zhou et al. [14]	1999	Voxel coding	SGI	NA	NA	✗	519
Ge et al. [5]	1999	3D topological thinning	SGI	NA	NA	✗	518(60†)
Horwich et al. [6]	1999	3D topological thinning	SGI	NA	1024	✓	<900
McFarland et al. [7]	1997	Radiologist marking	NA	NA	NA	✗	1080

† centreline calculation time obtained through using subsampling.

Table 1. An overview of previously published centreline calculation algorithms

can be either user defined [9] or automatically detected [13, 10]. We employ a modified version of 3D region growing for segmentation. The region growing process is initiated from an automatically detected seed point in the rectum (EP_{rec}) and the modification facilitates automated detection of a point in the caecum (EP_{cae}).

4. Centreline Calculation

We propose a fully automated centreline calculation algorithm based on 3D topological thinning as described by Tsao and Fu [11]. Centreline calculation using this approach is accurate, however, it has been discounted by others due to its computationally intensive nature [1, 9, 14]. Our novel approach enhances standard 3D topological thinning by employing optimisation techniques, thus significantly increasing performance. This performance increase is achieved without compromising accuracy.

Ge et al. [5] describe centreline calculation using 3D topological thinning as the removal of successive layers of surface voxels until certain topological and geometric constraints are violated. The topological constraints require that both the structure (number of holes) and connectivity of the object being thinned are preserved. The geometric constraints require that all skeleton endpoints are preserved. The thinned colon lumen may contain extraneous loops due to holes in the original binary model. These extraneous loops must be identified and removed in order to generate the final centreline.

4.1. Geometry Preservation

The geometric constraints associated with standard 3D topological thinning require that the skeletal endpoints of the object being thinned are retained. The modified region growing technique described in Section 3 identifies the only two endpoints of interest (i.e. the ultimate endpoints of the centreline EP_{rec} & EP_{cae}) thus substantially simplifying the task of geometric violation testing.

4.2. Connectivity Preservation

While thinning, the removal of a surface voxel (deletion candidate) must not affect the connectivity of the binary object being thinned. Connectivity can be tested at a local level by ensuring that the number of distinct binary objects in the $3 \times 3 \times 3$ neighbourhood centred around the deletion candidate does not increase due to the deletion of the centre voxel. We test for local connectivity breaches using a 3D labelling algorithm. If the number of labelled objects in the local $3 \times 3 \times 3$ neigbourhood increases after the removal of a deletion candidate then a local connectivity violation will be generated. If this is the case then the deletion candidate cannot be removed. The concept of local connectivity violation testing is illustrated in Figure 1.

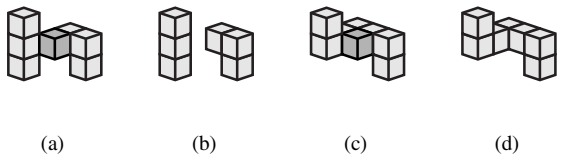

Figure 1. Examples where removal of the centre voxel generates a connectivity violation (a) & (b) and preserves connectivity (c) & (d).

4.3. Structure Preservation

Simply avoiding connectivity violations is not sufficient to guarantee the generation of a valid skeleton for a 3D object. It is possible to introduce an unwanted hole by deleting a voxel that does not generate a local connectivity violation. If this occurs then the topology of the object that is being thinned is altered. It is possible to detect the introduction of new holes at a local level by examining the $3 \times 3 \times 3$ neigbourhood centred about the current deletion candidate. The

Proceedings of the First International Symposium on 3D Data Processing Visualization and Transmission (3DPVT'02)
0-7695-1521-5/02 $17.00 © 2002 IEEE

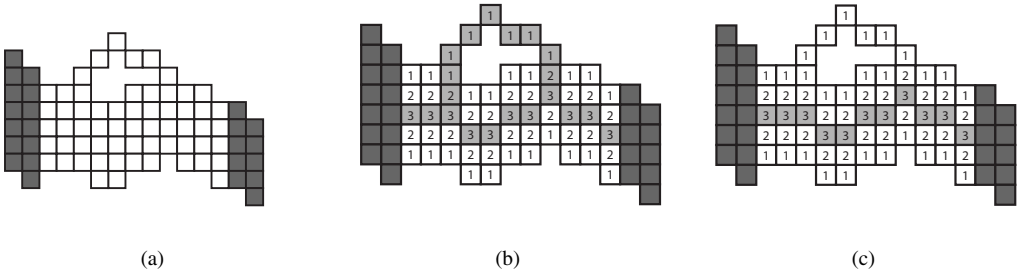

(a) (b) (c)

Figure 2. Extraneous loop removal illustrated using a 2D object (a). After thinning and distance field generation (b). After removal of extraneous loops as outlined in Section 4.4 (c).

test for the introduction of new holes is significantly more complex and time consuming than the test for local connectivity violations. The concept of hole detection is illustrated in Figure 3.

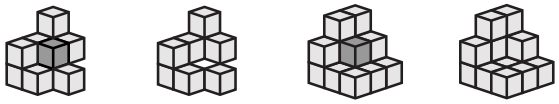

(a) (b) (c) (d)

Figure 3. Examples where removal of the centre voxel introduces a hole (a) & (b) and does not introduce a hole (c) & (d).

4.4. Extraneous Loop Removal

In some cases standard 3D topological thinning of the colon lumen does not generate the final centreline. The reason for this is that the calculated centreline includes extraneous loops. These loops are due to holes that are present in the original binary object being thinned. In the case of the colon lumen holes are normally present and are caused by folds in the colonic mucosa. Because of the local geometric constraints placed on the thinning algorithm these holes are retained in the final centreline in the form of extraneous loops. Extraneous loops can be removed by examining each centreline voxel and sequentially removing the voxels closest to the surface. A voxel must not be removed if it causes a global connectivity violation. This can be checked after the removal of each voxel by ascertaining whether or not a path exists between the EP_{cae} and the EP_{rec}. This process is outlined in Figure 2.

5. Optimisation

The task of topology preservation (Sections 4.2 & 4.3) is extremely inefficient. This Section describes two optimisation techniques which dramatically increase the performance of centreline calculation without compromising the accuracy of the result.

5.1. Surface Voxel Tracking

The thinning process only examines surface voxels. A surface voxel is a lumen voxel which is directly connected to a background voxel. Repetitive raster scanning of the entire volume to identify surface voxels is unnecessary. We propose a technique similar to that described by Ge et al. [5] for tracking surface voxels. Using this technique a single raster scan of the entire volume is performed to identify the initial set of surface voxels. The subsequent search for new surface voxels is restricted to the directly connected neighbours of previously deleted voxels. This optimisation technique significantly reduces the amount of data processing required compared with the standard raster scan based approach.

5.2. Partial Precalculation of Results

In order to increase the performance of the local neighbourhood analysis we precalculate the deletion value $d_i(X)$ of the centre voxel for each possible $3 \times 3 \times 3$ binary neighbourhood. The centre voxel in a $3 \times 3 \times 3$ neighbourhood has 26 neighbours. Each of these neighbour voxels is binary and as a result there can be 67,108,864 (2^{26}) possible neighbourhood configurations. Each of these neighbourhood configurations is generated and tested using the techniques outlined in Sections 4.2 & 4.3. The test results are stored in a lookup table. The unique index into this table for each neighbourhood is calculated using equation 1, $d_i(X)$ represents the

deletion value, i represents the neighbour index and $I(n)$ represents the value of the neighbour at index n.

$$d_i(X) = \sum_{n=1}^{26} 2^{n-1} I(n) \quad (1)$$

6. Results

We have performed initial tests using 5 CTC datasets obtained from the Department of Radiology in the Mater Misericordiae Hospital, Dublin, Ireland. All algorithms were implemented using Java and executed on a standard PC with a 700Mhz Intel PIII processor and 512MB of RAM. Segmentation and automatic endpoint detection were successful in all cases. centreline calculation was then performed, requiring an average of 24.42 seconds. A rendering of the colon centreline is presented in Figure 4.

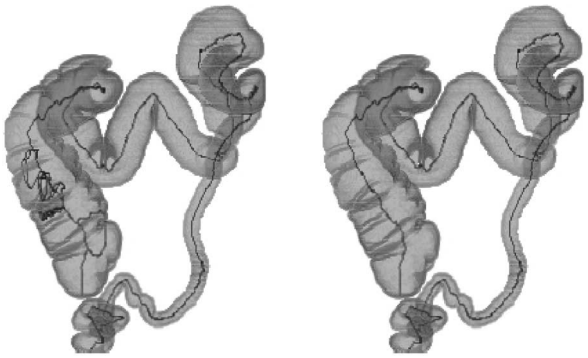

(a) (b)

Figure 4. A volumetric rendering of the colon lumen with centreline both before (a) and after (b) extraneous loop removal.

7. Conclusions

This paper describes an extremely efficient algorithm for calculating the centreline of the human colon for use with CTC. This technique uses automatically detected centreline endpoints, thus, no user interaction is required. Optimisation techniques that significantly increase the performance of 3D topological thinning are employed, however, these optimisation techniques do not compromise the accuracy of the resulting centreline. Our technique is fast, portable and robust while requiring a relatively modest hardware platform for execution. The results obtained from initial tests carried out on real patient data compare quite favorably with previously published results (see Table 1).

Acknowledgements

The authors wish to thank members of the Department of Radiology and the Gastrointestinal Unit at the Mater Misericordiae Hospital, particularly Dr. John Bruzzi, Dr. Helen Fenlon, Dr. Alan Moss and Dr. Padraic MacMathuna.

References

[1] I. Bitter, A. Kaufman, and M. Sato. Penalized-distance volumetric skeleton algorithm. *IEEE T Vis Comput Gr*, 7:195–206, 2001.

[2] D. Chen, B. Li, Z. Liang, M. Wan, A. Kaufman, and M. Wax. Tree-branch-searching multiresolution approach to skeletonization for virtual endoscopy. In *Proc. SPIE, Medical Imaging 2000: Image Processing*, volume 3979, pages 726–734, 2000.

[3] R. Chiou, A. Kaufman, Z. Liang, L. Hong, and M. Achniotou. An interactive fly-path planning using potential fields and cell decomposition for virtual endoscopy. *IEEE T Nucl Sci*, 46:1045–1049, 1999.

[4] T. Deschamps and L. Cohen. Fast extraction of minimal paths in 3D images and applications to virtual endoscopy. *Med Image Anal*, 5:281–299, 2001.

[5] Y. Ge, D. Stelts, J. Wang, and D. Vining. Computing the centerline of a colon: A robust and efficient method based on 3D skeletons. *J Comput Assist Tomo*, 23:786–794, 1999.

[6] P. Horwich, D. Chen, B. Li, M. Wax, G. Gindi, and J. Liang. The centerline of the colon: Automating a key step in virtual colonoscopy. *Radiology*, 213P:Suppl:691, 1999.

[7] E. McFarland, G. Wang, J. Brink, D. Balfe, J. Heiken, and M. Vannier. Spiral computed tomographic colonography: Determination of the central axis and digital unraveling of the colon. *Acad Radiol*, 4:367–373, 1997.

[8] NCRI. *Cancer in Ireland, 1997: Incidence and mortality*. Healy & Associates, 2000.

[9] Y. Samara, M. Fiebich, A. Dachman, J. Kuniyoshi, K. Doi, and K. Hoffmann. Automated Calculation of the Centerling of the Human Colon on CT Images. *Acad Radiol*, 6:352–359, 1999.

[10] M. Sato, S. Lakare, M. Wan, A. Kaufman, and M. Wax. An automatic colon segmentation for 3D virtual colonoscopy. *IEICE T Inf Syst*, E84D:201–208, 2001.

[11] Y. Tsao and K. Fu. A parallel thinning algorithm for 3-D pictures. *Comput Vis Graph Image Proc*, 17:315–331, 1981.

[12] D. Vining, D. Gelfand, R. Bechtold, E. Scharling, E. Grishaw, and R. Shifrin. Technical feasibility of colon imaging with helical CT and virtual reality. *Am J Roentgenol*, 162:Suppl:104, 1994.

[13] C. Wyatt, Y. Ge, and D. Vining. Automatic segmentation of the colon for virtual colonoscopy. *Comput Med Imag Grap*, 24:1–9, 2000.

[14] Y. Zhou and A. Toga. Efficient skeletonization of volumetric objects. *IEEE T Vis Comput Gr*, 5:196–209, 1999.